



Effect of lubricated-end-platens on the behavior of cemented paste backfill under triaxial loading

M. Jafari, M. Shahsavari & M. Grabinsky
Department of Civil Engineering – The University of Toronto, Toronto, Ontario, Canada

ABSTRACT

One of the most important factors that affects the behavior of Cemented Paste Backfill (CPB) under triaxial loading mode is the effect of stress non-uniformities during the test. In the triaxial test using the fixed ends, the stress and strain distributions are not uniform through the specimen which makes the interpretation of the data difficult. In this study, to overcome this issue and study the behavior of Cemented Paste Backfill (CPB) at large strains, two lubricated-end-platens were designed and fabricated. The results achieved from triaxial tests with lubricated-end platens on CPB specimens at different curing times prove the applicability of lubricated-end platens in minimizing the deformation non-uniformity in large strains.

RÉSUMÉ

Un des facteurs les plus importants qui affecte le comportement de remblai à pâte cimenté (RPC) sous chargement triaxial pendant les essais est le caractère non uniforme des contraintes. La distribution de contrainte-déformation n'est pas uniforme aux essais triaxiaux qui emploient des plaques d'extrémité fixées, ce qui rend l'interprétation des données difficile. Dans la présente étude, deux plaques aux extrémités lubrifiées ont été conçues et fabriquées afin de surmonter ces difficultés et de permettre l'étude de RPC soumis à une large déformation. Les résultats atteints des essais triaxiaux sur des échantillons de RPC durcies à périodes diverses démontrent l'applicabilité des plaques lubrifiées pour la minimisation de non uniformité dans les larges déformations.

1 INTRODUCTION

The triaxial specimen is assumed to be a uniform element of soil and therefore, any non-uniformity in the specimen detracts from this element assumption. There are several issues in conventional compression triaxial testing in which the non-uniform deformation through the specimen can be mentioned as the important one. In general, non-uniform deformation may develop due to the effect of end restraint, formation of shear bands under compression loading or specimen necking under extension loading. This non-uniformity can severely affect stress-strain and pore pressure uniformity through the specimen. The effect of deformation non-uniformity may be neglected in small strains while, at larger strains, definitely is the source of major errors (Rowe and Barden 1964, Sheahan 1991).

In the triaxial test using the fixed end (the ends of the specimen cannot deform freely in the radial direction), the stress and strain distribution are not uniform through the specimen which causes barreling effect and the concentration of dilation in local zones. The reason of this non-uniformity is related to the Poisson effect. Indeed, the end restraint causes higher stresses at the ends of the specimen comparing to the middle of that. This effect creates a zone called dead zone in which the end restraint affects the stress state.

Another effect of end restraint on the specimen is pore pressure non-uniformity. As mentioned before, the end restraint causes having higher radial stress at the specimen ends comparing the middle during undrained shear loading. The increase of the radial stress in the ends of the specimen reduces the shear stress and changes the pore pressure comparing the middle part of the specimen. The middle third of the specimen has mostly a uniform stress-strain state (if no pore water migration occurs);

however, in the conventional triaxial test, during the undrained shear, pore pressure measured at the base of the specimen is in the dead zone.

Pore pressure gradients in the specimen cause migrating pore water from one part of the specimen to another; this pore water migration can be observed more in over-consolidated soils. For example, in the slow test, the dilation at the middle third of specimen causes pore water migrates from ends to the middle of the specimen. This can be proven by measuring the water content of the middle and ends of the specimen after terminating the test.

Based on the above issues, it seems the true measure of stress and pore pressure in the drained and undrained response of the soil under triaxial test at the large strains is a difficult task. Sheahan (1991) classified the attempts to have more accurate measurements of pore water pressure into the following three groups:

- Reducing the testing rates: This gives sufficient time to pore pressure to be equalized through the specimen so that the reliable effective stress can be achieved by measuring the base pore pressure; the drawback is that the water migration is not prevented and the behavior is not completely undrained in undrained tests.

- Reading the specimen mid-height pore pressure: Some researchers used this method to determine the pore pressure in the specimen. In some cases, the pore pressure probe caused some soil disturbance since the probe should be inserted into the specimen, while some researchers have used a special type of probe in which the pressure transducer is placed on the surface of the soil specimen and does not disturb specimen (Thu et al. (2006)). At high strain rate, pore water can migrate through the specimen in the case of constraint end and also the sealing of the pore pressure probe in long-term tests can

be difficult. It is worth mentioning that this method can be used in low strain rate tests.

- Minimization of the triaxial specimen non-uniformities: pore water does not migrate through the specimen and pore pressure in the middle and ends are the same. Using lubricated-ends to decrease radial stresses at the ends of the specimen causes to have a more uniform specimen during the test. This helps to reduce the intensity of the dead zone and consequently, the pore pressure at the base is close to the middle. The interesting part of this attempt is that if the lubricated-end platens are completely effective in eliminating non-uniformities, no pore water migration happens and base pore water pressure can be used for any strain rate. Also, the shorter specimen can be tested using the lubricated-end platens which reduces the testing time needed for the pore pressure to be uniform in the specimen.

The lubricated-end platen introduced by Rowe and Barden (1964) has been accepted as an effective method to reduce the end restraint effect and minimize the deformation non-uniformity in the triaxial specimen. Inspired from Rowe's method, many researchers studied the effect of the lubricated-end platen and compared the results with end restraint tests in the triaxial specimen (Roy and Lo 1971, Tatsuoka et al. 1984, Ueng et al. 1988, Lo and Wardani 2002, Omar and Sadrekarimi 2014). They concluded that use of enlarged 'lubricated' end platens leads to a much greater uniformity of stress, deformation, and particle crushing throughout the specimen, and allows the specimen to retain its cylindrical shape even at large strains.

The lubricated-end triaxial tests mostly have been conducted on sand and applicability of this method on different soils and especially cemented soils have not been studied, comprehensively. In this study, a comprehensive set of tests has been conducted on Cemented Paste Backfill (CPB) with different cement contents under different curing times. The lubricated-end method was used in all of the tests and here the effect of this method on the uniformity of deformation through the specimen along with the effect of area correction methods on the mechanical parameters of this material are discussed.

3 EXPERIMENTAL PROGRAM

3.1 Triaxial compression testing equipment

A series of monotonic triaxial tests were performed using a combination of servo-hydraulic triaxial machine manufactured by Geotechnical Consulting and Testing Systems (GSTC) and a 50kN loading frame manufactured by the ELE Company. The main reason behind using the ELE loading frame instead of GCTS was related to the load fluctuation observed in the primary test results conducted using the GCTS loading frame with a very low displacement rate. In this study, the drained test was conducted with a displacement rate of 0.024 mm/min. The GCTS loading frame was designed for cyclic tests and this frame is not suitable for such low displacement rate tests.

In addition, a GCTS triaxial cell, manufactured from stainless steel, was used in this study. The top and bottom platens of this triaxial cell were modified to reduce end-

resistant effect and improve the uniformity of the specimen during large strain deformation. These new stainless steel platens had 91.5 mm diameter and a porous stone with a diameter of 25.4 mm was embedded in the middle of each platen to allow drainage from both sides. In addition, two sheets of latex membrane with 0.3 mm thickness and 77 mm diameter with a hole in the middle (for drainage purpose) were placed on both sides of the specimens. A thin layer of silicon lubricant was smeared between the latex membranes to reduce specimen end effects. In this study, the diameter of the specimen was 76.2 mm and the ratio of 1:1 between height and diameter of the specimen was considered.

The features of the sensors used in this study can be articulated as follows. The load cell has the capacity of $\pm 22000 \pm 2$ N; the LVDT has a range of 25.000 ± 0.005 mm displacement; and the pore pressure and cell pressure sensors have 1000 ± 1 kPa limits.

The Volume Change Device (VCD) used in this study is a frictionless rolling diaphragm type designed by GCTS with 0.01 ml resolution. VCD resolution enabled volumetric strain measurements to the nearest 0.002%. All sensors were calibrated before the testing program.

3.2 Material Description

The materials used in this study are Williams mine tailings, Portland cement, and mine process water. Mine tailing mainly consists of silicates, such as quartz, feldspar, and plagioclase, with traces of barite. To determine the grain size distribution of the tailings, sieve analysis and hydrometer test (ASTM C136-06 and ASTM D422-63, respectively) with a deflocculating agent were used and the result is presented in Figure 1. In addition, Portland cement (Canadian Standards Association (CSA) type 10 from Lafarge, Canada) used in this study. The density and specific surface of the Portland cement are 3.15 gr/cm^3 and $0.365 \text{ m}^2/\text{gr}$, respectively (Klein and Simon 2006).

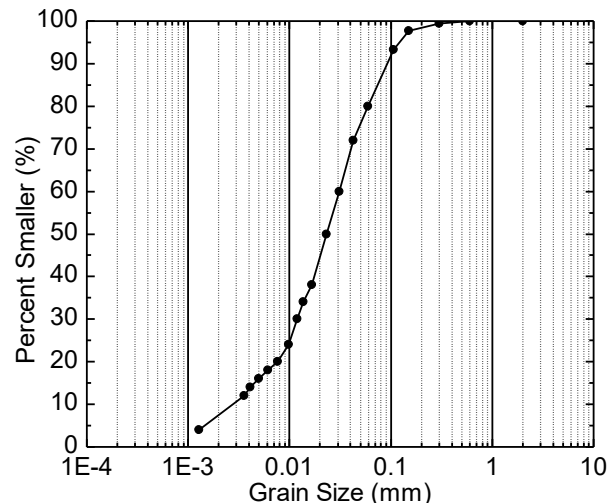


Figure 1. Grain-size distribution of the mine tailing

3.3 Specimen preparation

One of the main challenges in the laboratory scale study of CPB is specimen preparation. Jafari et al. (2017)

performed an extensive study on different specimen preparation techniques for CPB. They concluded the main problems associated with CPB specimen preparation (which has significant fractions of fines) as: (1) segregation of particles especially in CPB specimens with considerable sand fraction; (2) non-uniformity in density and void ratio along the specimen height; (3) large air bubbles trapped in specimens that reduce the degree of saturation and disturb the uniformity; and (4) non-uniformity in spatial distribution of cement particles. To have a uniform void ratio along the specimens, in this study, the method proposed by the mentioned authors were used. Based on their method of specimen preparation, first, the mine tailings were mixed with process water in a separate bucket for 15 minutes to ensure that the material was well blended. The water content of the mixture was determined accurately afterward. Based on the water content of the mixture, cement, water (if needed), and mine tailings values were determined and mixed with the desired water content. 3, 5, and 7% powdered Portland cement by weight of dry tailing was added to the mixture. In this procedure, the constituents were mixed continuously for 10 minutes using an electric hand mixer and no sign of segregation was observed. Water content was then measured before casting into the split mould.

The split mould has 76.2 mm diameter and 86 mm height as is shown in Figure 2. Combination of O-Rings at the top and bottom of the specimen associated with O-ring cord along the split mould grooves prevents any water loss during specimen preparation and its curing time. CPB specimens were cast into this mould on three layers. A glass rod with 5 mm diameter was used to spear each layer around 20 times to remove large entrained air voids. The specimens were cured under the water for the different curing times of 3, 7, 14, and 28 days. The specimens cast and prepared in the mentioned mould had very smooth end surfaces. In addition, to make sure about the smoothness of both ends of the specimen, each end of the specimens was polished on a glass surface before conducting the test.

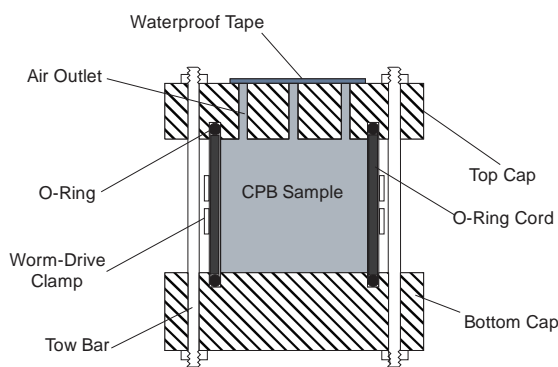


Figure 2. A schematic view of a designed split mould for lubricated-end triaxial specimen preparation

4 RESULTS AND DISCUSSIONS

In this paper, the results of Specimens with 5% cement content and 14 days curing time under different confining pressures are reported. Figure 3 (a) and (b) presents the q

and volumetric strain change versus axial strain in these tests. The abbreviations in the legend of the figure mean CC: Cement Content; CT: Curing Time; and CP: Effective Confining Pressure. As can be expected, the deviatoric stress increases by the increase of the effective confining pressure. Also, some strain softening can be observed after reaching the peak deviatoric stress. This strain softening behavior is more distinct in lower confining pressure. Moreover, axial strain at failure increases by the increase of the effective confining pressure (as can be observed in Figure 3 (a)).

Figure 3 (b) shows the volumetric response of material under different effective confining pressures. As can be observed, a similar pattern such as deviatoric response can be identified for a volumetric response. In all tests, the material shows a contractive behavior at the beginning along with dilatant behavior near to the failure. In lower effective confining pressures, the response is more dilatant; while, by an increase of confining pressure, the material shows more contractive behavior.

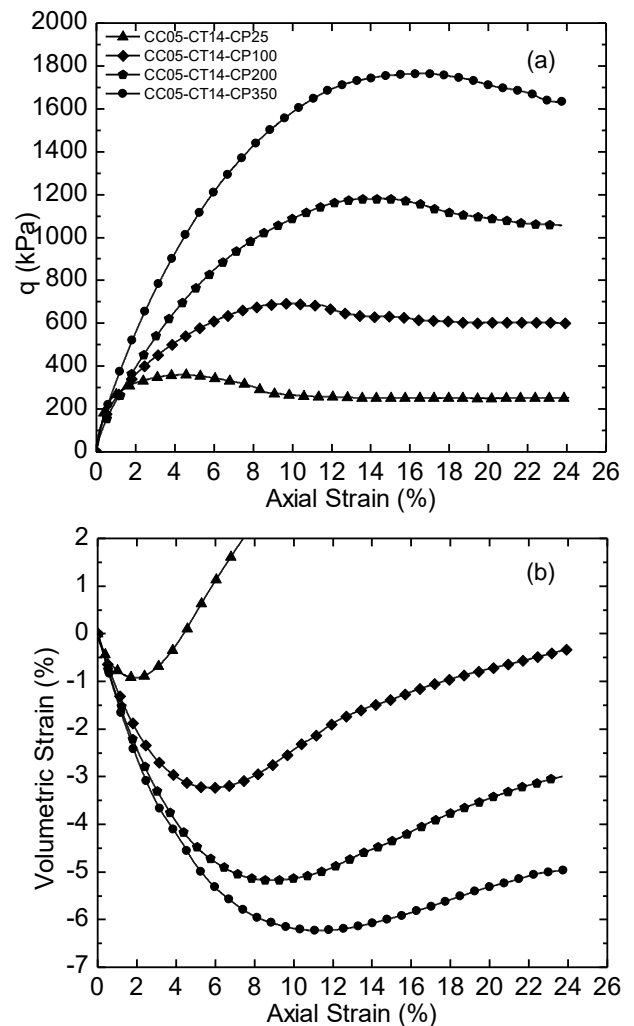


Figure 3. Triaxial response of CPB; (a) q vs axial strain; (b) volumetric vs axial strain

To study the effect of lubricated-end technique on the deformation uniformity of specimen testing, a webcam was placed in front of the specimens to automatically take the photos in the different strains during the triaxial test. Figure 4 and 5 show the deformation pattern in two of the specimens (with 25 and 350 kPa effective confining pressures, respectively) in the different strains. By interpreting all photos of specimens under different effective confining pressures, this can be concluded that all specimens remained cylindrical until failure. In lower

effective confining pressure (25 kPa), the material shows non-uniformity in lower axial strain (higher than 8%); however, for the rest of effective confining pressure, this non-uniformity happened in axial strains higher than 17%. Also, some specimens retained uniform deformation even in 20% axial strains as can be observed in Figure 5 (e).

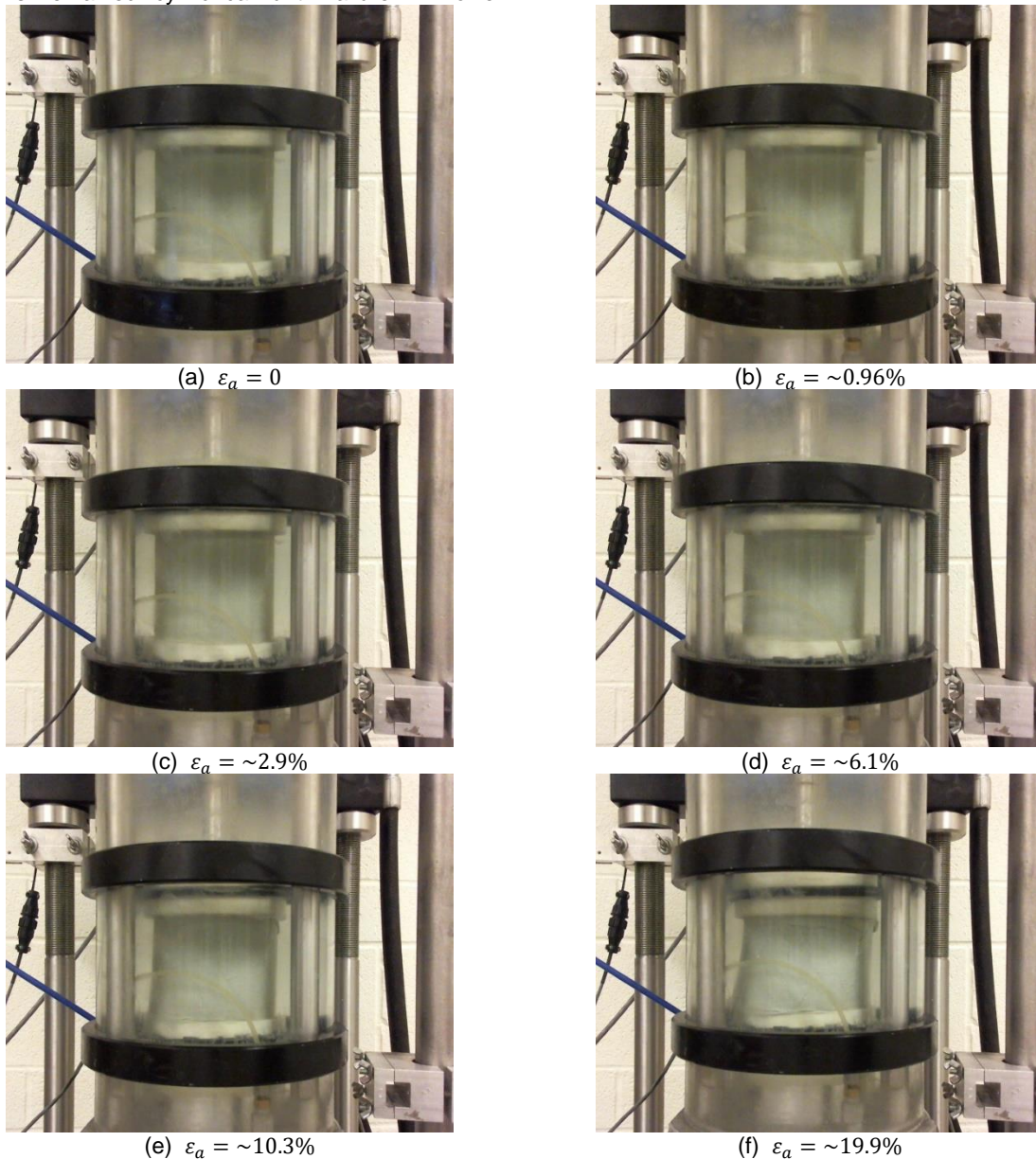


Figure 4. Photos of CC05-CT14-CP25 specimen during shearing stage (ε_a : axial strain)

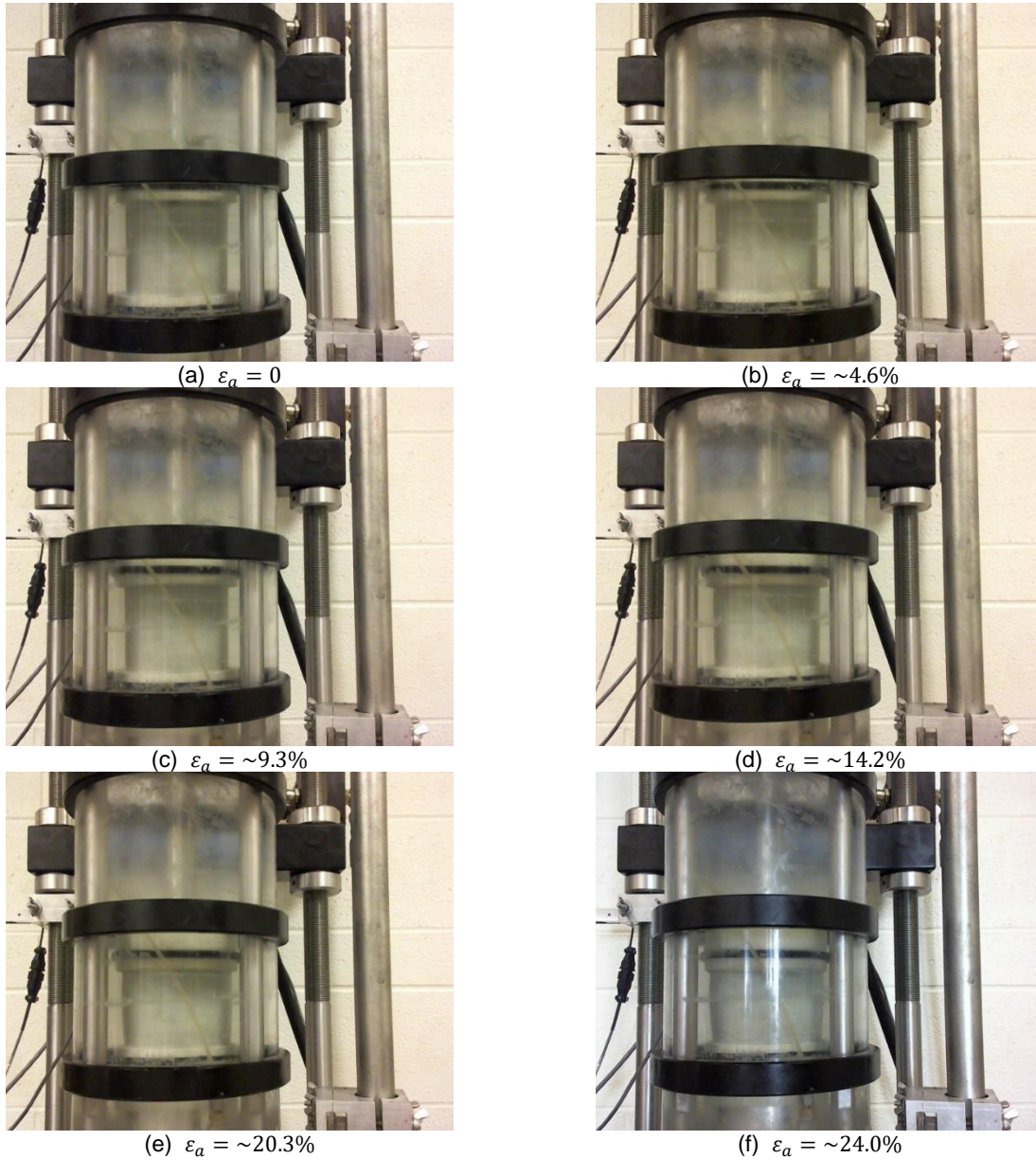


Figure 5. Photos of CC05-CT14-CP350 specimen during shearing stage (ϵ_a : axial strain)

4.1 Effect of different area correction methods on axial stress calculation

To study the behavior of soils such as steady state or post-peak state, it is necessary to shear the specimen to large axial strains. A triaxial soil specimen (especially for sand) may significantly show bulging deformation at large strains. The reason behind the bulging deformation is related to the specimen end restraint. This bulging deformation makes the calculation of the cross-sectional area difficult and consequently may result in errors in deviatoric stress calculation (which is axial load divided by the cross-sectional area of the specimen).

Many researchers observed bulging even in a triaxial test using lubricated-ends. It should be mentioned that most of the research has been conducted on sands and unfortunately, there has been little research on the behavior of cemented soils and the effect of lubricated-ends on the uniformity of deformation in the specimen. Several methods have been developed to calculate the cross-sectional area during the shearing stage. The choice of proper method should be based on observation of the profile of specimen deformation during the test. In this study, following three common methods of area correction were used:

- Cylindrical method:

This method has been accepted widely and traditionally has been used in the calculation of effective cross-sectional area in the specimen. The cross-sectional area is calculated by assuming that the specimen deforms uniformly along the height; on the other word, the specimen deforms as a right circular cylinder. Based on this method, the cross-sectional area, A , is determined as:

$$A = A_0 \left(\frac{1 - \varepsilon_v}{1 - \varepsilon_a} \right) \quad (1)$$

where, A_0 is the cross-sectional area of the specimen after consolidation stage; ε_v and ε_a are the volumetric and axial strain of the specimen, respectively (Donaghe et al. (1988)).

- Parabolic correction:

In large strains, specimen bulging due to end restraint causes the cross-section area to be larger than the overall average area. In this case, the parabolic correction can be used. This method has been developed explicitly for undrained condition and assumes that the specimen deforms as a parabola. This area correction can be formulated as:

$$A = A_0 \left[-\frac{1}{4} + \frac{\sqrt{25 - 20\varepsilon_a + 5\varepsilon_a^2}}{4(1 - \varepsilon_a)} \right]^2 \quad (2)$$

Although this method has been developed for the undrained test, here for sake of comparison, this method has been used as well.

- Zhang (1997) method:

Zhang (1997) investigated the deformation through the sand specimens and developed a method to correct the cross-sectional area in the specimens. They marked different heights of the triaxial specimens and measured the diameter in each marked points under different axial strains. As expected, they found the maximum diametric deformation occurred at the middle of the specimen and also, by compiling the results achieved in different marked points at different strains, they noticed that the specimen diameter changes with the height parabolically. Based on their experimental observations, they assumed that the diameters at both ends of the specimen are the same and developed the following equation for middle half average diameter, $D_{1/2}$:

$$D_{1/2} = D_m - \frac{1}{12} (D_m - D_0) \quad (3)$$

$$D_m = \frac{D_0}{4} \left(\sqrt{\frac{30(1 - \varepsilon_v)}{(1 - \varepsilon_a)} - 5} - 1 \right)$$

Where D_0 and D_m are the initial diameter of the specimen and maximum diameter for a given axial strain, respectively.

Figure 6 shows the deviatoric stress calculated by three different area correction methods. As can be seen, in both effective confining pressures, compared to the results with no area correction, all area correction methods reduced the deviatoric stress level.

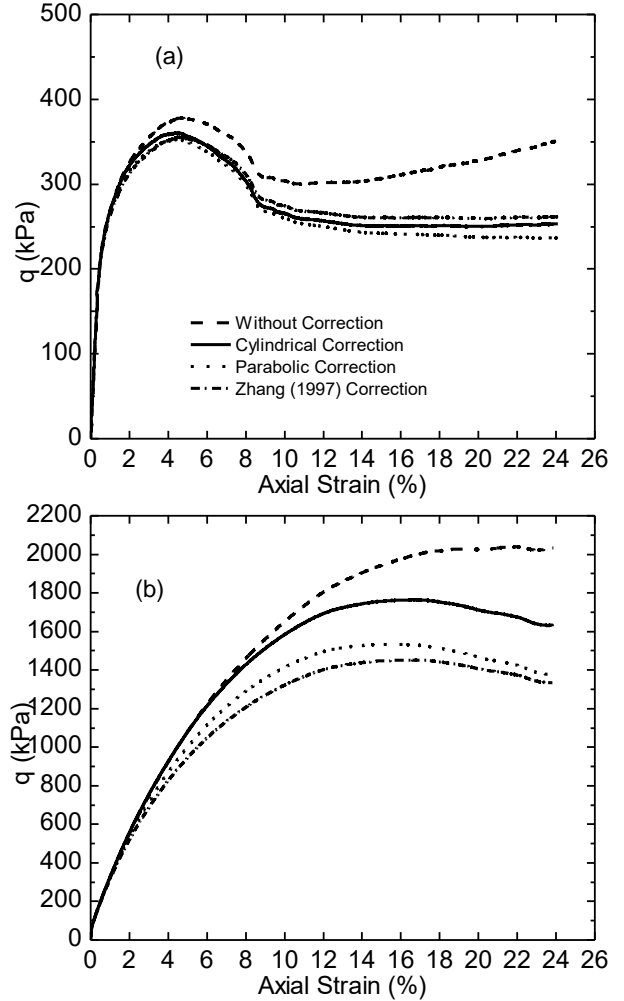


Figure 6. Effect of different area correction methods on Deviatoric stress of (a) CC05-CT14-CP25; and (b) CC05-CT14-CP350

To investigate the effect of area correction methods on the cohesion and internal friction angle, the deviatoric stress values at failure for different effective confining pressures were determined for each area correction method. Considering Mohr-Coulomb criterion:

$$q = \frac{2c \cos \phi}{1 - \sin \phi} + \frac{1 + \sin \phi}{1 - \sin \phi} \sigma_3 \quad (4)$$

where c and ϕ are cohesion and internal friction angle at the failure, respectively and σ_3 is the effective confining pressure. Figure 7 presents the extracted values at the failure for each area correction method. Based on the linear relation that can be observed for all methods, calculated cohesions and internal friction angles are presented in Table 1.

Study of the photos taken from varieties of specimens under different cement contents, curing times, and effective confining pressures shows that the CPB specimen deforms as a right circular cylinder using lubricated-end technique; this proves that the cylindrical cross-sectional area correction is the best method to calculate the deviatoric

stress. Compared to the cohesion and internal friction angle calculated using the cylindrical method, these parameters are significantly affected by the method of area correction. These differences show that choosing a proper method in cross-sectional area calculation is so important and the best method should be considered by investigating the deformation profile of the specimen through its height during the test.

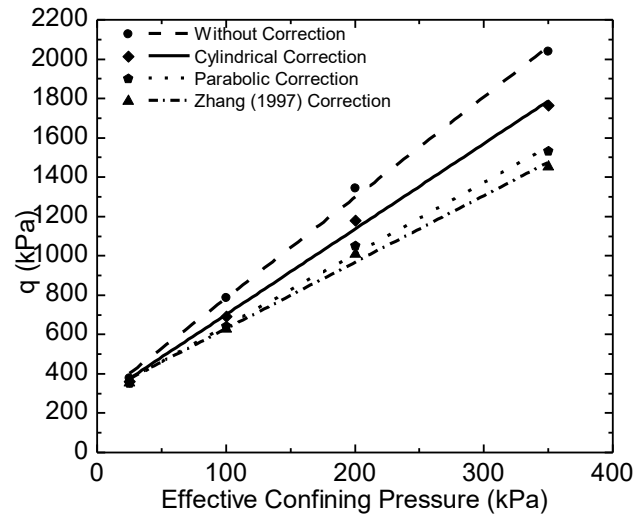


Figure 7. q versus effective confining pressure

Table 1. Mohr-Coulomb criterion parameters calculated for different area correction methods

Correction Method	Cohesion (kPa)	Friction angle (°)
Without Correction	60.56	42.30
Cylindrical	64.07	38.72
Parabolic	73.47	34.70
Zhang (1997)	79.15	32.94

5 CONCLUSION

Different triaxial tests were conducted on CPB with different cement contents and under varieties of curing times. The lubricated-end technique was implemented in these tests to study the large strain behavior of this cemented soil. The photos captured during tests from the specimens show that all specimens retained the uniform deformation not only until the failure level but also at large strains. This proves that the best method to correct the cross-sectional area is the traditional cylindrical method for CPB triaxial specimens.

6 REFERENCE

ASTM C136-06. 2006. Standard Test Method for Sieve Analysis of Fine and Coarse Aggregates, ASTM International.

ASTM D422-63. 2007. Standard Test Method for Particle-Size Analysis of Soils, ASTM International.

Donaghe, R. T., Chaney, R. C. and Silver, M. L. 1988. Advanced Triaxial Testing of Soil and Rock. 1916 Race Street, Philadelphia, PA, ASTM.

Jafari, M., Shahsavari, M. and Grabinsky, M. 2017. Cemented Paste Backfill Laboratory study: Sample preparation challenges. *GeoOttawa*. Ottawa.

Klein, K. and Simon, D. 2006. Effect of specimen composition on the strength development in cemented paste backfill, *Canadian Geotechnical Journal*, 43(3): 310-324.

Lo, S. R. and Wardani, S. P. 2002. Strength and dilatancy of a silt stabilized by a cement and fly ash mixture, *Canadian Geotechnical Journal*, 39(1): 77-89.

Omar, T. and Sadrekarimi, A. 2014. Specimen size effects on behavior of loose sand in triaxial compression tests, *Canadian Geotechnical Journal*, 52(6): 732-746.

Rowe, P. W. and Barden, L. 1964. Importance of free ends in triaxial testing, *ASCE, Journal of the Soil Mechanics and Foundations Division*, 90(No. SM1): 1-27.

Roy, M. and Lo, K. Y. 1971. Effect of End Restraint on High Pressure Tests of Granular Materials, *Canadian Geotechnical Journal*, 8(4): 579-588.

Sheahan, T. C. 1991. An experimental study of the time-dependent undrained shear behavior of resedimented clay using automated stress path triaxial equipment, Massachusetts Inst. of Technol., Cambridge, Mass. ScD thesis.

Tatsuoka, F., Molenkamp, F., Torii, T. and Hino, T. 1984. Behavior of lubrication layers of platens in element tests, *SOILS AND FOUNDATIONS*, 24(1): 113-128.

Thu, T. M., Rahardjo, H. and Leong, E.-C. 2006. Shear Strength and Pore-Water Pressure Characteristics during Constant Water Content Triaxial Tests, *Journal of Geotechnical and Geoenvironmental Engineering*, 132(3): 411-419.

Ueng, T., Tzou, Y. and Lee, C. 1988. The effect of end restraint on volume change and particle breakage of sands in triaxial tests. *Advanced Triaxial Testing of Soil and Rock*, ASTM.

Zhang, H. 1997. Steady state behavior of sands and limitations of the triaxial tests, University of Ottawa, Ottawa, Canada. PhD.